

Magnetic Measurements of the First Nb₃Sn Model Quadrupole (MQXFS) for the High-Luminosity LHC

J. DiMarco, G. Ambrosio, G. Chlachidze, P. Ferracin, E. Holik, G. Sabbi, S. Stoynev, T. Strauss, C. Sylvester, M. Tartaglia, E. Todesco, G. Velez, X. Wang

Abstract— The US LHC Accelerator Research Program (LARP) and CERN are developing high-gradient Nb₃Sn magnets for the High Luminosity LHC interaction regions. Magnetic measurements of the first 1.5 m long, 150 mm aperture model quadrupole, MQXFS1, were performed during magnet assembly at LBNL, as well as during cryogenic testing at Fermilab's Vertical Magnet Test Facility. This paper reports on the results of these magnetic characterization measurements, as well as on the performance of new probes developed for the tests.

Index Terms— High Luminosity LHC, Field Quality, Magnetic Measurements, High Field Nb₃Sn Magnet.

I. INTRODUCTION

In support of the high luminosity upgrade of the Large Hadron Collider, the LHC Accelerator Research Program (LARP) and CERN are developing large aperture high-field quadrupoles based on Nb₃Sn technology to be used in the interaction regions [1]. MQXFS1a is a 1.5-meter long, 150 mm diameter aperture Nb₃Sn short model quadrupole of the same design that will be used for eventual production of these magnets. A detailed description of the magnet design can be found elsewhere [2]. The magnet was assembled at LBNL using coils fabricated at Fermilab and BNL, and first cryogenic tests have been recently completed at Fermilab [3]. This paper reviews the magnetic measurements performed at LBNL and Fermilab's Vertical Magnet Test Facility (VMTF) and discusses some results pertaining to magnet and measurement quality. Additional field quality analysis can be found in another paper at this conference [4].

II. PROBES AND MEASUREMENT SYSTEMS

Magnetic measurements of MQXFS1a were performed with Printed Circuit Board (PCB) rotating coil probes [5], the technique having been validated throughout the HQ magnetic measurement program [6,7]. These PCB probes are of radial type, with 5 different loops (one is a spare) side to side across the board, each with 12 turns per layer, and trace separation 0.35 mm. To provide a high-sensitivity harmonics measurement having Un-Bucked (UB), Dipole-Bucked (DB), and Dipole-Quadrupole-Bucked (DQB) signals, the loops are combined in an analog bucking configuration via jumpers on the board. Two types of board were developed: the first was a 2-layer design with circuits having their longest traces as 55 mm and 110 mm;

the other was a 30-layer design with longest traces being 110 mm and 220 mm long (see Fig. 1). A cross-section of the 30-layer probe is shown in Fig. 2.



Fig. 1 Circuit board probes used for the measurements. Top: the 55 mm/110 mm 2-layer PCB; bottom: the 220 mm/110 mm 30-layer PCB.

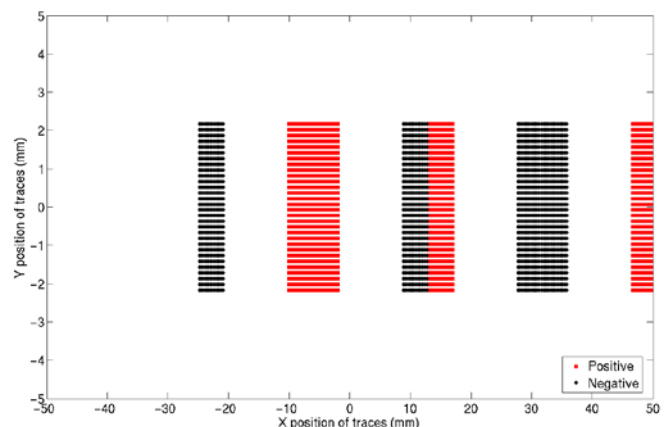


Fig. 2 Cross-section of the 30-layer printed circuit board used in the probe. The thickness is 4.5 mm and the width is about 80 mm (95 mm including the spare loop (not shown)).

The 110 mm and 220 mm probe lengths roughly correspond to integer multiples of the 109 mm twist pitch of the Rutherford superconductor cable used in the coils while the 55 mm probe length allows us to see the size of variations in the harmonics if only half the twist pitch length is covered. Because of the probe ends, the effective lengths in terms of integrated harmonic field was 106.7 mm for the 110 mm probe. Therefore performing a set of axial measurements with this step size provides a summation which does not have overlap or gaps. For the 220 mm probe, the corresponding step is 216.7 mm. The board is

Manuscript received September 2, 2016. This work was supported by the U.S. Department of Energy through the US LHC Accelerator Research Program (LARP) and by the High Luminosity LHC project.

G. Chlachidze, G. Ambrosio, J. DiMarco, E. Holik, S. Stoynev, T. Strauss, C. Sylvester, M. Tartaglia, G. Velez are with Fermi National Accelerator

Laboratory, Batavia, IL 60510, USA (J. DiMarco phone: +1-630-840-2672; fax: +1-630-840-8079; e-mail: dimarco@fnal.gov).

G.L. Sabbi, X. Wang are with Lawrence Berkeley National Laboratory, Berkeley, CA 94720, USA.

P. Ferracin and E. Todesco are with CERN, TE Dept. CH-1211 Geneva.

positioned with respect to its end plugs via 3D-printed support pieces. The completed VMTF probe is shown in Fig. 3.

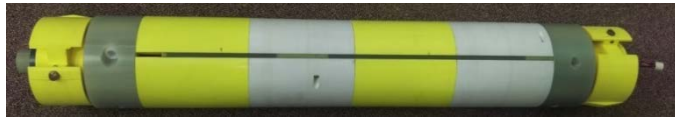


Fig. 3 The full probe assembly with bearings used at VMTF

For the measurements during assembly at LBNL, the entire aperture is available for the magnetic measurement device except for a few mm of radial space used for instrumentation such as strain gauges and spot heaters and their wiring. To avoid interfering or damaging this instrumentation, a support tube for the probe of OD 125 mm and ID 120 mm was inserted through the magnet and centered at its ends. A portable rotating coil system, a so-called FERRET [5], having a self-contained rotating PCB probe and encoder and external non-magnetic flexible drive shaft was fabricated for these measurements. The nominal rotation radius available to the FERRET probe was 59.5 mm, and so was ~20% larger than the 50 mm reference radius. The PCB board (2-layer, 110 mm long) was identical to the one used for cold measurements, but installed at the larger radius, thus providing very high sensitivity. The LBNL measurements also employed the on-board amplifier circuitry included on the PCB. Axial motion of the probe relied on a measurement tape attached to the probe and so had limited accuracy. Data acquisition used a NI4462 24-bit ADC as described in [8]. The probe rotation rate was 3Hz.

The probe radius for the cold measurements was constrained by the 103.5 mm ID of the new anti-cryostat optimized for MQXF testing. A nominal rotation radius of 50.75 mm was selected to allow clearance of the rotating probe within the anti-cryostat, the probe being centered by means of spring-loaded bearings at each end. The sensitivity factors (K_n) for the 30-layer 100 mm probe at Fermilab are shown in Fig. 4 along with those of the 2-layer probe – the increase in sensitivity of the LBNL configuration for high orders is of course due to its larger measurement radius. For axial positioning the VMTF vertical drive uses a screw-driven rail with precision of 10 μ m. The FNAL data acquisition was DSP-based [9] with 16-bit ADCs. Rotation speed was 1Hz for the VMTF measurements.

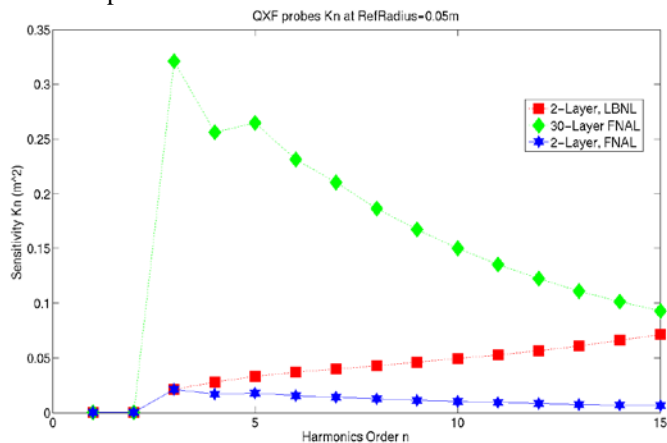


Fig. 4 Sensitivity factors for the probes used at FNAL and LBNL

An in-situ calibration procedure [10] was applied to determine the actual radial position of the PCB and the offset

distance of its plane to the rotation axis. For the LBNL FERRET probe, this showed that the actual radial position was smaller than nominal by 30 μ m and the shift of the PCB in the direction normal to its planar surface was 60 μ m. The 30-layer probe at Fermilab had actual radius about 0.28 mm larger than nominal and planar shift of about 50 μ m. These values were incorporated in the analysis.

Resolution of the probe is estimated based on comparison to expected harmonic fall-off from Biot-Savart considerations [11]; this is shown for the 110 mm-long probes at LBNL and Fermilab in Figs. 5-6. For the LBNL warm measurements the resolution was ~0.003 units at the 50mm reference radius, while for the warm measurements at FNAL with the 2-layer probe the resolution was ~10-20 times larger. This difference can be attributed to the larger measurement radius at LBNL; if the reference radius is set to the probe radius, the resolution is comparable to that at FNAL. Also, interestingly, the 30-layer probe warm measurements at FNAL gave very similar results as the 2-layer, which during cold measurements at 17.7 kA were only a factor 2-3 better than its warm result. These indicate that resolution is limited by factors other than signal size.

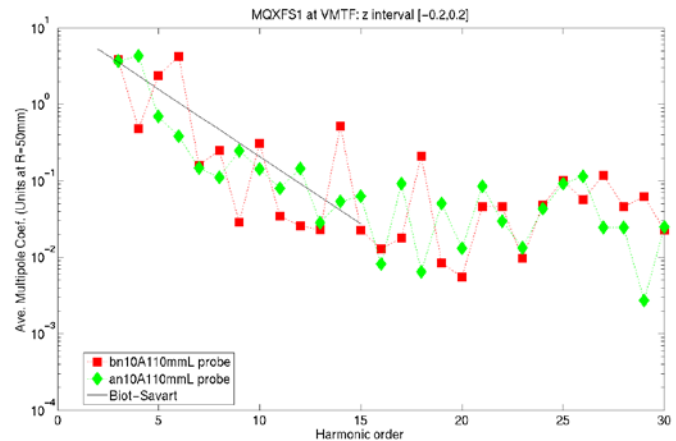


Fig. 5 Probe resolution for VMTF probe at room temperature.

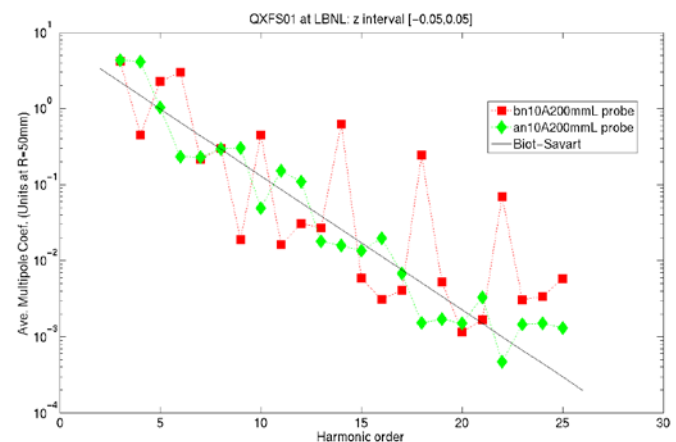


Fig. 6 Probe resolution for the FERRET probe at LBNL

Some mechanical issues with the bearings were resolved in preparation for the next test campaign (designated MQXFS1b), ongoing at the time of this writing. A comparison of the warm resolution before and after this mechanical optimization will allow a check of whether resolution improved because of these reasons.

There were also issues with the large signal sizes of the 30-layer probe in the first thermal cycle stemming from the use of attenuators in the data acquisition. Starting in the second thermal cycle, we switched to the lower sensitivity, 2-layer boards to avoid the large signal sizes and ADC saturation altogether, and most of the data here are from this probe. The use of the 30-layer probe will also be revisited for MQXFS1b.

III. MAGNETIC MEASUREMENTS

The magnetic field in the aperture of the quadrupole is expressed in terms of harmonic coefficients defined in a series expansion using the complex function formalism

$$B_y + iB_x = B_2 10^{-4} \sum_{n=1}^{\infty} (b_n + ia_n) \left(\frac{x + iy}{R_{ref}} \right)^{n-1} \quad (1)$$

where B_x and B_y in (1) are the horizontal and vertical field components in the Cartesian coordinates, b_n and a_n are the normalized $2n$ -pole normal and skew harmonic coefficients in "units" at the reference radius $R_{ref} = 50$ mm [12]. The right-handed magnet coordinate system is shown in Fig. 7 viewing the magnet from the lead end. The Z-axis zero position is at the center of the magnet pointing from return to lead end.

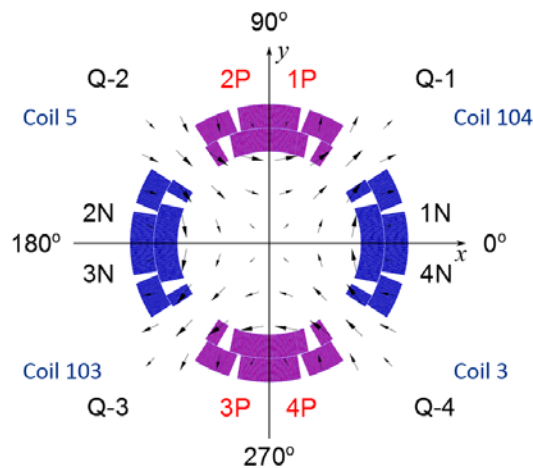


Fig. 7 Coordinate system definition for MQXFS1. Coils 3 and 5 were built by LARP and 103 and 104 by CERN. The 'P' and 'N' represent regions with positive and negative currents directed along +Z respectively.

Measurements made at room temperature combined +/- currents to remove magnetization effects. Measurements at 1.9K included axial scans, simulated accelerator cycles, and ramp rate and 'stairstep' loops [13].

Average straight-section magnet harmonics ($z = -0.3$ m to 0.2 m) at various z -scan currents are shown in Table I. Note that the magnet combined two pairs of coils built with different conductor and tooling (one pair fabricated by LARP and one by CERN). Ref [4] provides a comparison of the measurements with calculations taking into account the as-built parameters. Table II provides some detail on coil differences.

Fig. 8 shows the warm/cold correlation of low-order harmonics. These are generally close (within ~ 1 unit) to unit slope, indicating that it should be possible to determine and try to compensate such geometrical effects before final assembly. An exception to this is a_4 , which shows a larger offset due to

asymmetric size differences among the coils used in MQXFS1 assembly [4]. The b_6 also has a significant offset.

TABLE I

AVERAGE STRAIGHT SECTION FIELD HARMONICS								
n	I=0.96 kA (1.9K)		I=6.0 kA (1.9K)		I=16.48 kA (1.9K)		I=17.8 kA (1.9K)	
	b_n	a_n	b_n	a_n	b_n	a_n	b_n	a_n
3	0.77	8.20	-3.94	2.93	-4.39	3.13	-4.43	3.23
4	0.13	-21.91	-0.08	-6.05	0.14	-6.80	0.10	-7.00
5	0.56	1.10	2.67	-0.95	2.75	-0.97	2.82	-1.03
6	-5.82	0.51	-0.52	0.48	0.68	0.44	0.61	0.46
7	-0.60	-0.56	0.19	0.22	0.19	0.26	0.17	0.32
8	0.32	-0.62	0.24	-0.66	0.24	-0.67	0.23	-0.72
9	0.45	0.02	0.21	0.29	0.22	0.31	0.23	0.31
10	1.63	0.08	-0.21	0.16	-0.46	0.15	-0.49	0.16
11	0.14	0.03	0.03	-0.10	0.04	-0.10	0.05	-0.09
12	-0.09	-0.24	-0.04	0.06	-0.03	0.06	-0.03	0.05
13	-0.06	0.07	0.03	0.05	0.03	0.05	0.02	0.04
14	-0.63	0.01	-0.81	0.02	-0.70	0.02	-0.70	0.01

TABLE II
MQXFS1 COILS

	Coil	Conductor	Core
LARP	3	108/127	10.1mm centered
LARP	5	108/127	11.9mm biased to thick edge
CERN	103	132/169	14mm, full coverage
CERN	104	132/169	14mm, full coverage

Magnet transfer function vs z is shown in Fig. 9. The effects of saturation at the higher currents are clear. The b_3/a_3 and b_4/a_4 vs axial position are shown in Fig. 10 and Fig. 11. These indicate some local conductor positioning errors during coil/magnet fabrication which vary along the magnet length. An effort to mitigate the average effect of these with full-length magnetic shims is being tested in the MQXFS1b test cycle.

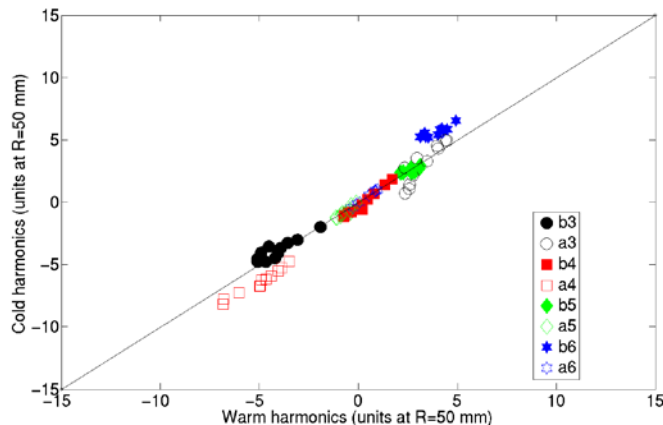


Fig. 8 Cold vs Warm harmonics correlation at multiple axial positions in the magnet straight section. Cold harmonics are taken at 16.48 kA but compensated so as to represent the cold geometric component for comparison to the warm data. That is, hysteresis, saturation, and persistent current effects present at the high current have been removed by comparing the up/down-ramp difference at 6000A (which gives the geometric harmonics) to the value at 16.48 kA (which includes the other effects). The up/down-ramp measurements were made at a single axial position (at center), but the correction has been applied along the entire straight section as these effects should not have strong axial dependence.

To estimate the effect of the eddy currents on the magnet field quality, several excitation loops have been performed at ramp rates of 13 A/s, 20 A/s, 40 A/s, and 80 A/s. The measured variation of the quadrupole transfer function (TF), and most other harmonics, as a function of the excitation current ramp rate is small, as expected because of the cored cable.

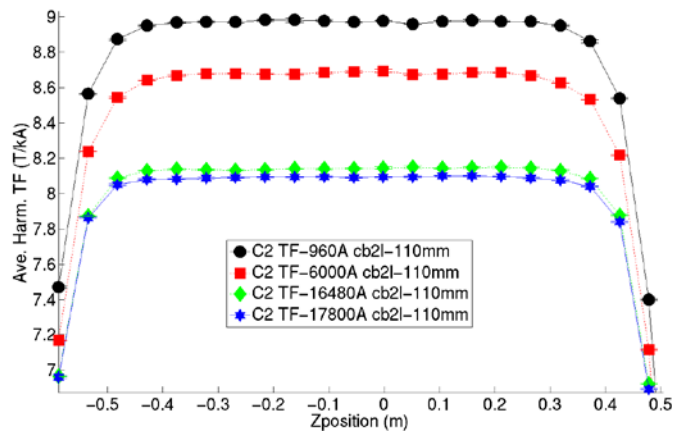


Fig. 9. Transfer function vs. axial position at various currents.

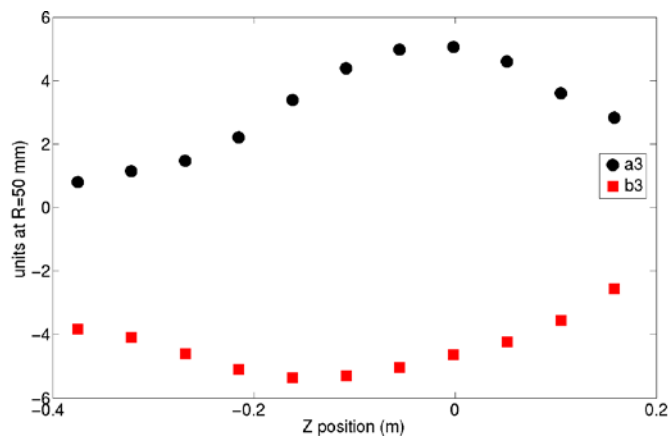


Fig. 10 Sextupole harmonics as a function of axial position in magnet straight section

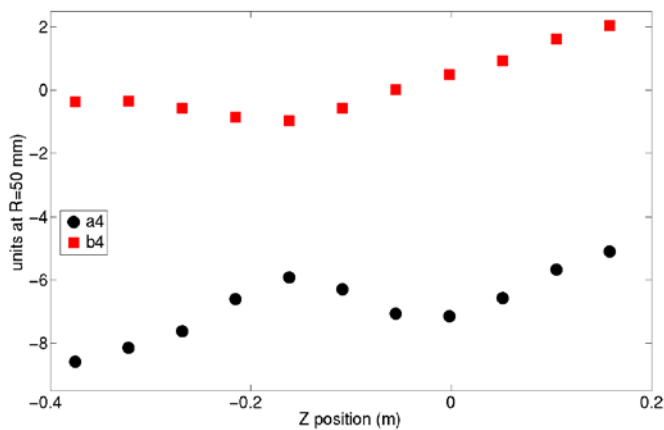


Fig. 11 Octupole harmonics as a function of axial position in magnet straight section

However, Figs. 12 and 13 show that the corresponding skew sextupole (a_3) and skew octupole (a_4) field loops have significant ramp rate dependence. The cause of the larger effect observed in these components is still being investigated, but that they arise in these harmonics is likely again connected with the different coils used in construction (e.g., the different core configurations shown in Table II). When ramping stops, these effects decay relatively quickly within ~4-5 s (Fig. 14).

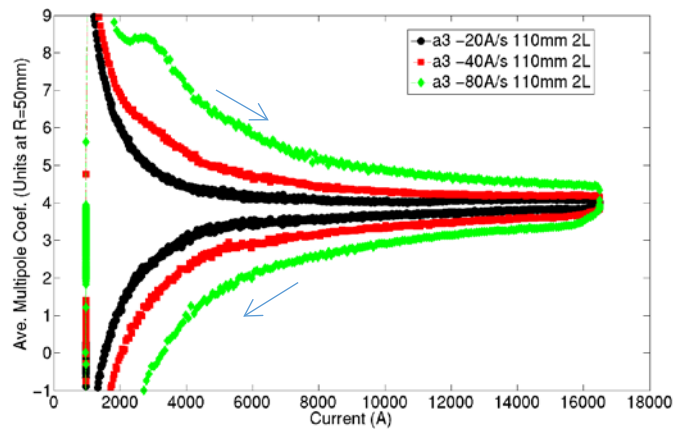


Fig. 12. a_3 vs. magnet current at var. ramp rates.

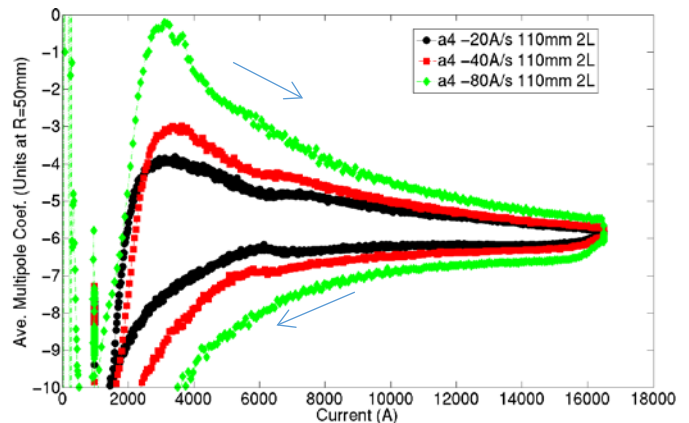


Fig. 13. a_4 vs. magnet current at var. ramp rates .

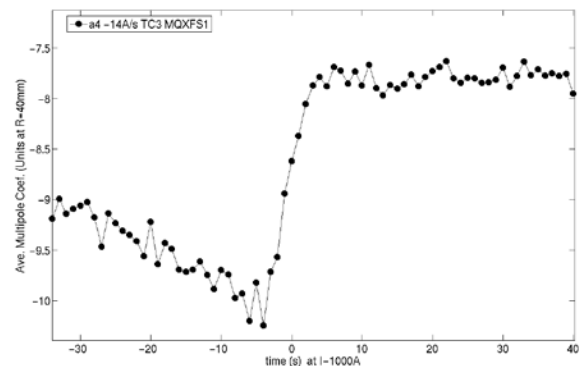


Fig. 14. a_4 vs. time during a stair-step measurement. The 1000A flattop current is reached at $t=0$, and the dynamic effects decay within a few seconds.

IV. CONCLUSION

MQXFS1 has been fabricated and has undergone a first set of magnetic measurements at the Fermilab Vertical Test Facility. The magnet performs well in terms of field uniformity and dynamic behavior, though low orders still have substantial axial variation and need to be tuned. The probes developed for these measurements have performed well, but required improvement of the initial rotation mechanics.

REFERENCES

- [1] E. Todesco, *et al.*, "Design studies for the low-beta quadrupoles for the LHC luminosity upgrade," *IEEE Trans. Appl. Supercond.*, vol 23, no. 3, p. 4002405, June 2013.
- [2] "HL-LHC Preliminary Design Report", CERN-ACC-2014-0300, 28 November 2014.
- [3] G. Chlachidze *et al.*, "Performance of the first short model 150 mm aperture Nb₃Sn quadrupole MQXFS for the High-Luminosity LHC upgrade", 1LOR3C-04, to be presented at this conference.
- [4] S. Izquierdo Bermudez *et al.*, "Magnetic Analysis of the Nb₃Sn low-beta Quadrupole for the High Luminosity LHC", 2LPo2B-09, to be presented at this conference.
- [5] J. DiMarco, *et al.*, "Application of PCB and FDM Technologies to Magnetic Measurements Probe System Development," *IEEE Trans. Appl. Supercond.* vol. 23, no. 3, pp. 9000505, Jun. 2013.
- [6] J. DiMarco, G. Ambrosio, M. Buehler *et al.*, "Field quality measurements of LARP Nb₃Sn magnet HQ02," *IEEE Trans. Appl. Supercond.*, vol. 24, no. 3, p. 4003905, 2014.
- [7] X. Wang, *et al.*, "Validation of Finite-Element Models of Persistent-Current Effects in Nb₃Sn Accelerator Magnets," *IEEE Trans. Appl. Supercond.*, vol. 25, no. 5, pp. 4003006, Jun. 2015.
- [8] X. Wang, *et al.*, "Summary of HQ01e magnetic measurements", LBNL report 5290E, Berkeley, CA, December 2012.
- [9] G. V. Velev, *et al.*, "A Fast Continuous Magnetic Field Measurement System Based on Digital Signal Processors," *IEEE Trans. Appl. Supercond.* vol. 16, no. 2, pp. 1374-1377, Jun. 2006.
- [10] J. DiMarco, *et al.*, "PCB Probe Development", Proceedings of the 18th International Magnetic Measurements Workshop, Brookhaven, NY, USA, 2013.
- [11] F. Borgnolutti, *et al.*, "Reproducibility of the Coil Positioning in Magnet Models Through Magnetic Measurements", *IEEE Trans. Appl. Supercond.*, vol. 19, no. 3, pp. 1100-1105, 2009.
- [12] A. Jain, "Basic Theory of Magnets", *Proc. CERN Accelerator School*, Anacapri, Italy, CERN-98-05, pp.1-26, 1997.
- [13] G. Sabbi, *et al.*, MQXFS1 run plan, <http://larpdocs.fnal.gov/LARP-public/DocDB/ShowDocument?docid=1079>